

Higgs Boson Interference in $\gamma\gamma \rightarrow W^+W^-$ D.A. Morris,^{a*} T.N. Truong^{b†} and D. Zappalá^{a‡}

^aUniversity of California, Los Angeles
405 Hilgard Ave., Los Angeles, CA, 90024 U.S.A.

^bCentre de Physique Théorique de l'Ecole Polytechnique,
91128 Palaiseau, France

Abstract

We study interference effects between resonant and nonresonant amplitudes for the $\gamma\gamma \rightarrow W^+W^-$ process at a backscattered photon-photon collider. We show that a Higgs boson with $M_H \gtrsim 200$ GeV is manifest as a resonant dip in the W^+W^- invariant mass spectrum and we investigate its statistical significance.

*email: morris@uclahep.bitnet

†email: pthtnt@frpoly11

‡email: zappala@uclahep.bitnet

There has been recent interest in weak gauge boson pair production in $\gamma\gamma$ collisions as a means of testing the Standard Model and studying a Higgs boson with a mass up to a few hundred GeV[1, 2, 3]. Photons with the necessary energies may be produced by backscattering low energy laser beams at future e^+e^- or e^-e^- facilities[3, 4, 5]. In this letter we examine the prospects for studying a Higgs boson with $M_H > 2M_Z$ through the process $\gamma\gamma \rightarrow H \rightarrow W^+W^-$ by investigating the role of quantum interference effects.

To lowest order, $\gamma\gamma \rightarrow H \rightarrow W^+W^-$ proceeds through the one-loop diagrams of Fig. 1a. However, due to a large background of nonresonant tree-level processes (see Fig. 1b), it has generally been concluded that the W^+W^- decay mode of a heavy Higgs boson would be difficult to exploit. $H \rightarrow ZZ$, which has no tree-level background, looks more promising in this respect[1, 3, 6, 7, 8, 9]. Unfortunately, cursory studies of the $H \rightarrow W^+W^-$ channel have neglected interference between the tree and loop amplitudes of Fig. 1: constructive interference effects could strengthen the viability of the W^+W^- mode. In this letter we report our findings of relatively large destructive interference effects in the $\gamma\gamma \rightarrow W^+W^-$ channel which imply that, in marked contrast to earlier studies, a Higgs boson of mass $M_H \gtrsim 200$ GeV is manifest as a resonant dip in the W^+W^- invariant mass spectrum.

We are interested in the process $\gamma\gamma \rightarrow W^+W^-$ in vicinity of a Higgs boson resonance (i.e., $|M_{WW} - M_H|/\Gamma_H \simeq \mathcal{O}(1)$ where M_{WW} is the W^+W^- pair invariant mass and Γ_H is the Higgs boson decay width). The relevant diagrams are shown in Fig. 1. For $M_{WW} = M_H$ the loop amplitudes of Fig. 1a are of $\mathcal{O}(\alpha)$ due to a cancellation of weak coupling constants between the HW^+W^- vertex, the $Hf\bar{f}$ vertex and Γ_H in the Higgs boson propagator. For $|M_{WW} - M_H|/\Gamma_H \gg \mathcal{O}(1)$ the loop amplitudes are $\mathcal{O}(\alpha\alpha_w)$ so that, strictly speaking, a complete calculation in this region should include $\mathcal{O}(\alpha\alpha_w)$ contributions from one-loop radiative corrections to the nonresonant tree amplitudes of Fig. 1b. We can safely neglect such corrections for our purposes since they are $\mathcal{O}(\alpha_w)$ smaller than the tree-level amplitudes and they vary smoothly over the interval $|M_{WW} - M_H|/\Gamma_H \simeq \mathcal{O}(1)$ where interference phenomenon occur.

The literature contains separate calculations for the helicity amplitudes corresponding to the loop diagrams of Fig. 1a [10] and the tree diagrams of Fig. 1b [11, 12]. Unfortunately, since such calculations do not chronicle their choice of phase conventions, it is impossible to combine the results of different authors with any degree of certainty. We have recalculated the helicity amplitudes of Fig. 1 using uniform

phase conventions and find complete agreement (modulo different phase transformations) with the amplitudes of Refs. [10, 12][§]. For completeness we list the relevant phase conventions and helicity amplitudes in the Appendix.

Fig. 2 shows the $\gamma\gamma \rightarrow W^+W^-$ cross section $\sigma_{\lambda\lambda'}$ for various Higgs boson masses as function of the $\gamma\gamma$ center of momentum energy $\sqrt{s_{\gamma\gamma}}$ where $\lambda, \lambda' = \pm$ denote the photon helicities. The cross sections are integrated over all scattering angles and summed over the polarization states of the W bosons. Though the overall magnitude of resonance phenomena decreases as M_H increases (due to Γ_H increasing), there is a trend suggesting overall destructive interference as M_H increases. Throughout this letter we use $M_Z = 91.17$ GeV, $M_W = 80.22$ GeV, $m_t = 150$ GeV and neglect threshold effects in the Higgs boson width and in the direct production of W boson pairs.

Let us investigate the extent to which the interference features of Fig. 2 survive in the environment of a $\gamma\gamma$ collider. Assuming that each $e^+(e^-)$ gives precisely one backscattered photon, the W^+W^- invariant mass spectrum at a backscattered $\gamma\gamma$ facility is given by

$$\frac{d\sigma}{dM_{WW}} = \frac{2M_{WW}}{s_{e^+e^-}} \sum_{\lambda\lambda'} \int \frac{dx}{x} d\cos\theta^* f_\lambda(x) f_{\lambda'}\left(\frac{M_{WW}^2}{xs_{e^+e^-}}\right) \frac{d\sigma_{\lambda\lambda'}}{d\cos\theta^*}, \quad (1)$$

where $f_\lambda(x)$ is the probability that laser photon backscatters to become a photon with helicity λ carrying a fraction x of the beam energy $\sqrt{s_{e^+e^-}}/2$. The precise form of $f_\lambda(x)$ depends on the degree of polarization of both the laser and the $e^+(e^-)$ beams. Efficiency considerations suggest[5] that the laser energy ω and the $e^+(e^-)$ beam energy be chosen in a manner such that the limits of integration become

$$x_{max} = \frac{2\omega\sqrt{s_{e^+e^-}}}{2\omega\sqrt{s_{e^+e^-}} + m_e^2} = .828, \quad x_{min} = \frac{M_{WW}^2}{x_{max} s_{e^+e^-}}. \quad (2)$$

The limits of integration over the W^+W^- center of mass scattering angle θ^* are functions of x and laboratory acceptance criteria.

For purposes of illustration, let us restrict our attention to an experimental arrangement in which completely circularly polarized laser photons (with helicities chosen so that $\lambda_1^{\text{laser}} = \lambda_2^{\text{laser}}$)** backscatter off completely unpolarized e^+e^- beams

[§]Due to an apparent inconsistency in the labeling of polarization vectors for transverse W bosons in Ref. [11], our tree amplitudes differ from those of Ref. [11] by more than a simple phase convention.

**The case $\lambda_1^{\text{laser}} \neq \lambda_2^{\text{laser}}$ gives less promising results which we do not present.

where $\sqrt{s_{e^+e^-}} = 500$ GeV. Explicit expressions for $f_\lambda(x)$ may be found in Ref. [4]. We should emphasize that we choose this arrangement primarily for its simplicity. We have made no attempt at optimizing the experimental arrangement since we simply wish to investigate the degree to which the resonant dip in the M_{WW} spectrum survives in a “typical” setup.

Figure 3a shows the W^+W^- invariant mass spectrum for various values of the Higgs boson mass; the spectrum corresponds to Eq. 1 multiplied by the square of the branching fraction $\text{Br}(W \rightarrow \text{hadrons}) \simeq .7$ since M_{WW} is most reliably reconstructed by requiring both W bosons to decay hadronically. Furthermore, we have required the laboratory angles of both the W^+ and W^- to obey^{††} $|\cos \theta_{\text{lab}}| < .85$. For comparison, the dashed line in Fig. 3a includes only the nonresonant tree-level background processes.

Due to imperfect mass reconstruction in an actual experiment, the distribution of the measured invariant mass of a W^+W^- pair, M_{WW}^{meas} , will differ from that shown in Fig. 3a. To simulate this effect we define “smeared” cross sections through convolution with a Gaussian resolution function,

$$\frac{d\tilde{\sigma}}{dM_{WW}^{\text{meas.}}} = \int dM_{WW} \frac{1}{\sqrt{2\pi}\sigma_{res}} \exp\left[-\frac{(M_{WW}^{\text{meas}} - M_{WW})^2}{2\sigma_{res}^2}\right] \frac{d\sigma}{dM_{WW}}, \quad (3)$$

where σ_{res} is the experimental resolution. Fig. 3b demonstrates how $\sigma_{res} = 5$ GeV smooths the details of the distribution shown Fig. 3a. The dashed line in Fig. 3b corresponds to smearing the tree-level background processes.

Let us investigate how the including interference effects changes the nature of the Higgs boson signal in the M_{WW} distribution. Suppose we define the Higgs boson signal S as the excess or deficit of W^+W^- pairs in a specific mass interval with respect to tree-level background expectations,

$$S = f \times \int dM_{WW}^{\text{meas}} \left(\frac{d\tilde{\sigma}}{dM_{WW}^{\text{meas}}} - \frac{d\tilde{\sigma}^{\text{tree}}}{dM_{WW}^{\text{meas}}} \right). \quad (4)$$

The factor f is the e^+e^- integrated luminosity which is appropriate since we assume each $e^+(e^-)$ gives exactly one backscattered photon. We will assume a yearly integrated luminosity of $f = 20 \text{ fb}^{-1}$ [1, 7] for our calculations. Similarly, we define the

^{††}Due to limitations in the computer time necessary to achieve acceptable statistics, we have compromised by imposing lab angle cuts on the W bosons rather than their jet decay products. It should be noted that authors sometimes impose angular cuts in the $\gamma\gamma$ center of mass frame which do not necessarily correspond to configurations accessible to experiments[1, 3, 7, 11].

background B as

$$B = f \times \int dM_{WW}^{meas} \frac{d\tilde{\sigma}^{\text{tree}}}{dM_{WW}^{meas}}. \quad (5)$$

The nature of the interference between the Higgs boson signal and the nonresonant background may be deduced from Fig. 4 which plots the fractional excess of W^+W^- pairs, S/B , as a function of M_H . For definiteness we choose an integration interval of $M_H \pm 2\Gamma_H$ in Eqs. 4,5 and assume perfect resolution ($\sigma_{res} \rightarrow 0$ GeV as in Fig. 3a). The net interference effect (after integrating over the chosen interval) is destructive beyond $m_H \gtrsim 200$ GeV. For comparison, the dashed line in Fig. 4 illustrates the inevitable fractional excess if one (incorrectly) combines the signal and background processes incoherently. The change of slope in both curves at $M_H = 2M_Z \simeq 182$ GeV is due to the $H \rightarrow 2Z$ threshold in the Higgs boson width.

We can go beyond the qualitative nature of Fig. 4 by considering the statistical significance of a Higgs boson signal in the $\gamma\gamma \rightarrow W^-W^+$ channel. If we wish to employ a simple $|S|/\sqrt{B}$ measure of statistical significance, it would clearly be unwise to restrict our attention to S defined over a M_{WW} bin centered on M_H as we did for Fig. 4 since such bins potentially encompass regions of both constructive and destructive interference. However, for a fixed binwidth one can optimize the position of the bin center to maximize $|S|/\sqrt{B}$; though such an optimization is statistically illegal (unless one compensates for the reduction in the number of degrees of freedom) we will nevertheless use this technique to place an upper limit on the significance attainable.

With the binwidth chosen as $\max(2\sigma_{res}, \Gamma_H)$, the solid curve in Fig. 5 plots the maximum $|S|/\sqrt{B}$ obtainable for $\sigma_{res} = 5$ GeV for the backscattered laser facility we consider. The dashed curve in Fig. 5 gives the value of $|S|/\sqrt{B}$ obtained in the spirit of previous analyses which a) neglect interference effects b) assume experimental resolution effects are accounted for solely by the binwidth (i.e., they impose no Gaussian smearing) and c) center the bins on M_H . Because of these differences the curves in Fig. 5 are not directly comparable: the dashed curve is included only for reference to previous studies. As in Fig. 4, there is a change in slope of the curves in Fig. 5 at $M_H = 2M_Z$ due to an abrupt change in the Higgs boson decay width (neglecting threshold effects).

Our motivation for pursuing the issue of interference effects in $\gamma\gamma \rightarrow H \rightarrow W^-W^+$ was the possibility that significant interference, if present, could brighten

the prospects for exploiting the W^+W^- mode for detecting a Higgs boson with $M_H > 2M_Z$ at a backscattered laser facility. We have demonstrated that the relevant interference terms can indeed be large and that for $M_H \gtrsim 200$ GeV they result in a net destructive interference which not only negates the contributions from an incoherent signal (i.e., from the square of the loop amplitudes) but also produces a net resonant dip in the corresponding M_{WW} spectrum: this is the central result of this letter. Unfortunately, the statistical significance of the resonant dip is not encouraging (at least in the experimental arrangement considered) and thus the W^+W^- mode for $M_H > 200$ GeV remains elusive even though the underlying nature of the signal is significantly altered.

We would like to thank B. Cousins and J. Hauser for enlightening discussions. D.A.M. acknowledges the hospitality of the S.S.C. Theory Group while part of this work was being completed. T.N.T. likewise acknowledges the U.C.L.A. Theory Group for an enjoyable visit. D.A.M. is supported by the Eloisatron project. D.Z. is supported by the I.N.F.N.

Appendix

For completeness, we summarize expressions for the relevant tree and loop amplitudes of Fig. 1. We use the Feynman rules listed in Ref. [13] and the phase conventions described below.

In the W^+W^- center of momentum system we define the contravariant components of the momentum and polarization vectors for the W^- boson as

$$p^\mu = (E, |\vec{p}| \sin \theta^*, 0, |\vec{p}| \cos \theta^*) \quad (6)$$

$$\epsilon_\pm^\mu = \frac{1}{\sqrt{2}}(0, \cos \theta^*, \pm i, -\sin \theta^*) \quad (7)$$

$$\epsilon_0^\mu = \frac{1}{M_W}(|\vec{p}|, E \sin \theta^*, 0, E \cos \theta^*) \quad (8)$$

where $E = \sqrt{|\vec{p}|^2 + M_W^2}$. The corresponding components for the W^+ boson are obtained by the substitution $\theta^* \rightarrow \pi + \theta^*$. The components for a photon traveling along the $+z$ ($-z$) axis follow from Eqs. 6,7 by substituting $\theta^* \rightarrow 0$ ($\theta^* \rightarrow \pi$), where $E = |\vec{p}|$ is understood.

The sum of the amplitudes corresponding to Fig. 1 may be written as

$$A_{\lambda_1\lambda_2\lambda_3\lambda_4} = A_{\lambda_1\lambda_2\lambda_3\lambda_4}^{\text{loop}} + A_{\lambda_1\lambda_2\lambda_3\lambda_4}^{\text{tree}} \quad (9)$$

where $\lambda_1, \lambda_2, \lambda_3, \lambda_4$ refer to the helicities of the photon along the $+z$ axis, the photon along the $-z$ axis, the W^- boson and the W^+ boson respectively.

The loop amplitudes may be expressed as

$$A_{\lambda_1\lambda_2\lambda_3\lambda_4}^{\text{loop}} = -\frac{\alpha g^2}{8\pi} \frac{(\epsilon_{\lambda_1} \cdot \epsilon_{\lambda_2})(\epsilon_{\lambda_3}^* \cdot \epsilon_{\lambda_4}^*)s}{s - M_H^2 + i\Gamma_H M_H} \times \left[3r_W(2 - r_W)G(r_W) + 3r_W + 2 - 2 \sum_f Q_f^2 r_f \{(1 - r_f)G(r_f) + 1\} \right] \quad (10)$$

where $r_i = 4M_i^2/s$ and the sum is over all massive fermions species (with charge Q_f in units of $|e|$), including color as a degree of freedom. The function $G(r)$ is given by

$$G(r) = \begin{cases} \frac{\pi^2}{4} - \frac{1}{4} \ln^2 \left(\frac{1 + \sqrt{1-r}}{1 - \sqrt{1-r}} \right) + \frac{i\pi}{2} \ln \left(\frac{1 + \sqrt{1-r}}{1 - \sqrt{1-r}} \right) & r < 1 \\ \left(\arctan \frac{1}{\sqrt{r-1}} \right)^2 & r > 1. \end{cases} \quad (11)$$

In our phase conventions the tree amplitudes which interfere with the loop amplitudes may be written as

$$A_{\lambda_1\lambda_2\lambda_3\lambda_4}^{\text{tree}} = \frac{8\pi\alpha}{1 - \cos^2\theta^* + r_W \cos^2\theta^*} \times \tilde{A}_{\lambda_1\lambda_2\lambda_3\lambda_4}^{\text{tree}}, \quad (12)$$

where

$$\tilde{A}_{++++}^{\text{tree}} = 2 \pm 2\sqrt{1 - r_W} - r_W, \quad \tilde{A}_{++00}^{\text{tree}} = r_W, \quad (13)$$

with $\tilde{A}_{\lambda_1\lambda_2\lambda_3\lambda_4}^{\text{tree}} = \tilde{A}_{-\lambda_1-\lambda_2-\lambda_3-\lambda_4}^{\text{tree}}$. All other tree amplitudes do not interfere with the loop amplitudes and hence their overall phases are irrelevant for our purposes. Explicit expressions for them may be found in Ref. [12].

References

- [1] J.F. Gunion and H.E. Haber, UCD preprint, UCD-92-22, August 1992.
- [2] D. Boswer-Chao and K. Cheung, Phys Rev. **D48**, (1993) 89.

- [3] D.L. Borden, D.A. Bauer, D.O. Caldwell, UCSB preprint UCSB-HEP-93-01, March 1993.
- [4] I.F. Ginzburg, G.L. Kotkin, V.G. Serbo and V.I. Telnov, Nucl. Inst. Meth. **205**, (1983), 47; I.F. Ginzburg, G.L. Kotkin, S.L. Panfil, V.G. Serbo and V.I. Telnov, Nucl. Inst. Meth. **219**, (1984), 5.
- [5] V.I. Telnov, Nucl. Instr. Meth. **A294**, (1990) 72.
- [6] G.V. Jikia, Phys. Lett. **B298** (1993) 224.
- [7] M. Berger, UW Madison preprint MAD/PH/771, July 1993.
- [8] D. Dicus and C. Kao, U. of Texas preprint CCP-93-24, August 1993.
- [9] H. Veltman, private communication to T.N.T.
- [10] A.I. Vainshtein, M.B. Voloshin, V.I. Zakharov and M.A. Shifman, Sov. J. Nucl. Phys. **30**, (1979), 711 [Yad. Fiz. **30**, (1979), 1368].
- [11] E. Yehudai, Phys. Rev. **D44**, (1991), 3434.
- [12] G. Belanger and F. Boudjema, Phys. Lett. **B288**, (1992), 210.
- [13] K. Aoki *et al.*, Supp. Prog. Theor. Phys., **73** (1982) 1.

Figure Captions

- Fig. 1** a) One loop diagrams for $\gamma\gamma \rightarrow H \rightarrow W^+W^-$. b) Nonresonant tree-level diagrams for $\gamma\gamma \rightarrow W^+W^-$.
- Fig. 2** Photon-photon cross sections for W pair production as a function of $\gamma\gamma$ center of mass energy $\sqrt{s_{\gamma\gamma}}$ and incoming photon helicities λ, λ' . For three values of the Higgs boson mass we show cross sections which have been integrated over all W^+W^- scattering angles and summed over W boson polarizations. Solid lines include interference effects between tree and loop amplitudes of Fig. 1. Dashed and dot-dashed lines include only tree level contributions.
- Fig. 3** (a) W^+W^- invariant mass spectrum at a $\sqrt{s_{e^+e^-}} = 500$ GeV backscattered laser facility with completely polarized lasers ($\lambda_1^{\text{laser}} = \lambda_2^{\text{laser}}$) and completely unpolarized $e^+(e^-)$ beams. Solid lines include interference between tree and loop amplitudes. Dashed line includes only nonresonant tree amplitudes. Perfect experimental resolution is assumed. (b) Same as in (a) except with $\sigma_{\text{res}} = 5$ GeV experimental resolution effects implemented.
- Fig. 4** Fractional excess of W^+W^- pairs in the M_{WW} interval $M_H \pm 2\Gamma_H$ assuming perfect experimental resolution at a $\sqrt{s_{e^+e^-}} = 500$ GeV backscattered laser facility with completely polarized lasers ($\lambda_1^{\text{laser}} = \lambda_2^{\text{laser}}$) and completely unpolarized $e^+(e^-)$ beams. Solid line includes interference between tree and loop amplitudes whereas dashed line neglects interference effects. The horizontal dotted line at $S/B = 0$ suggests that net interference effect is destructive for $m_H \gtrsim 200$ GeV.
- Fig. 5** Statistical significance of Higgs boson signal in the W^+W^- invariant mass spectrum at a $\sqrt{s_{e^+e^-}} = 500$ GeV backscattered laser facility with completely polarized lasers ($\lambda_1^{\text{laser}} = \lambda_2^{\text{laser}}$) and completely unpolarized $e^+(e^-)$ beams. An integrated e^+e^- luminosity of 20 fb^{-1} is assumed. The binwidth for both curves is fixed at $2\sigma_{\text{res}} = 10$ GeV. The solid curve includes interference effects, $\sigma_{\text{res}} = 5$ GeV resolution effects, and corresponds to an optimized bin center. The dashed curve neglects interference effects and assumes resolution effects are accounted for solely by the binwidth with bins centered on M_H .

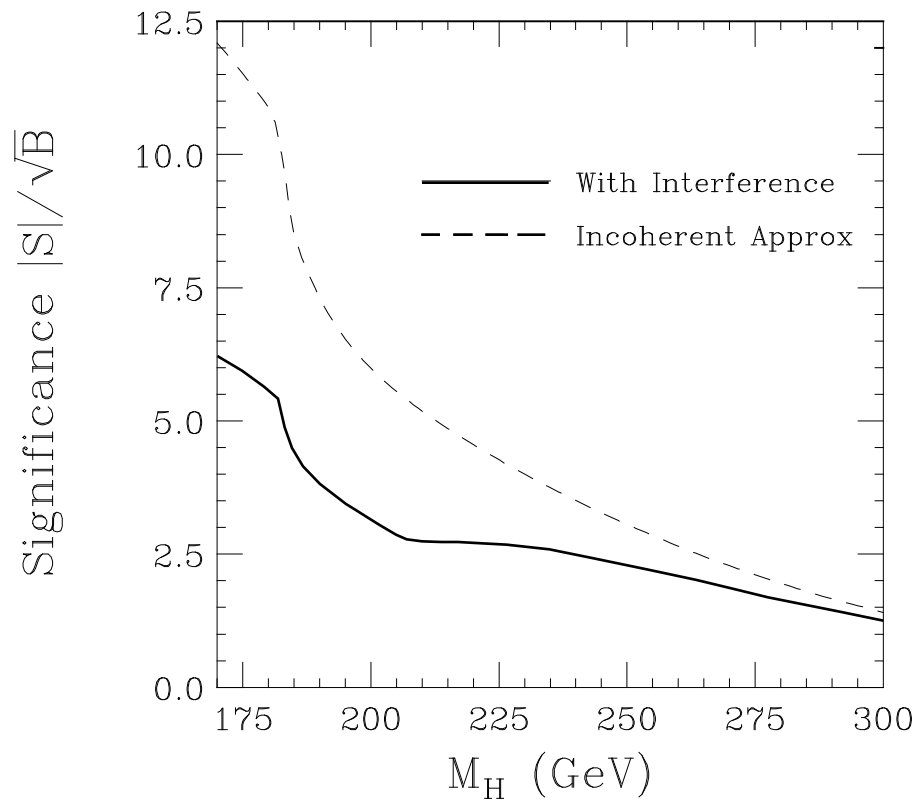


Figure 5

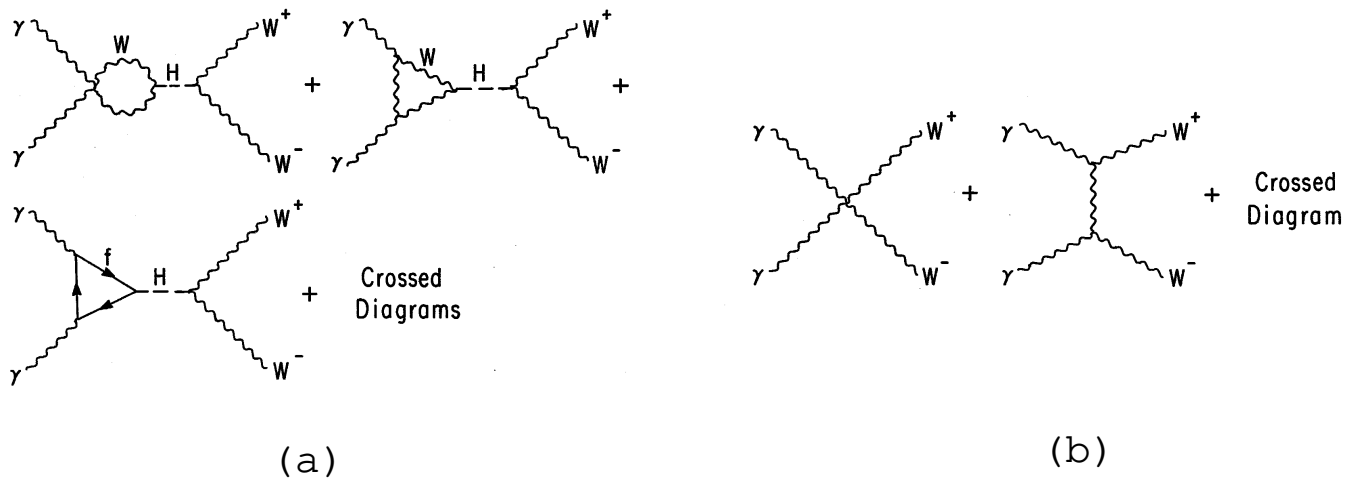


Figure 1

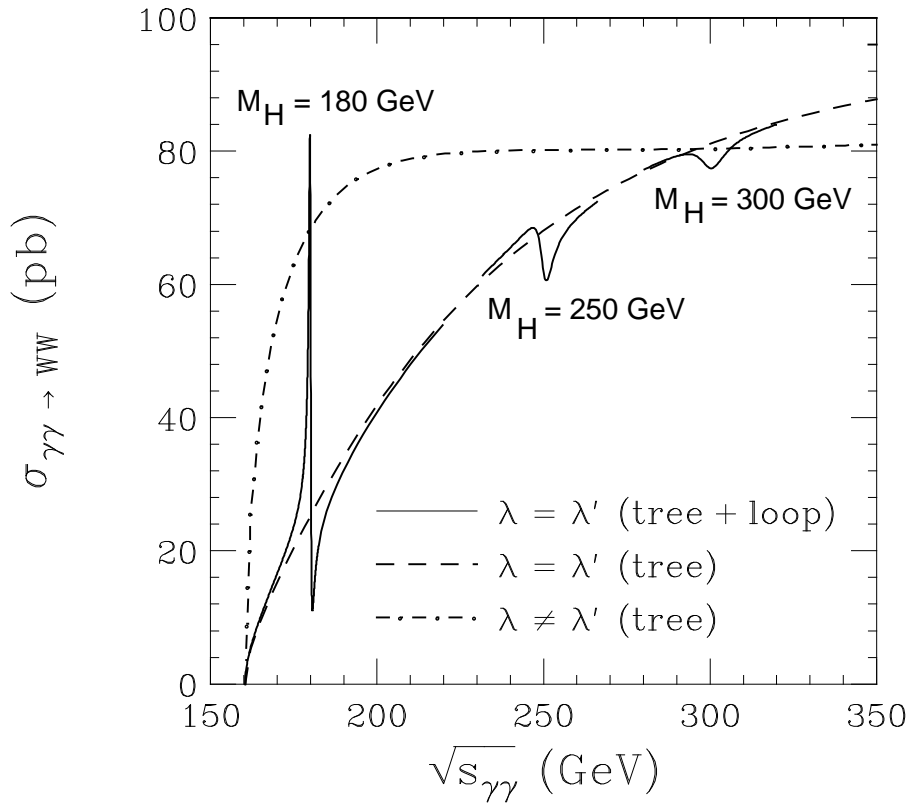


Figure 2

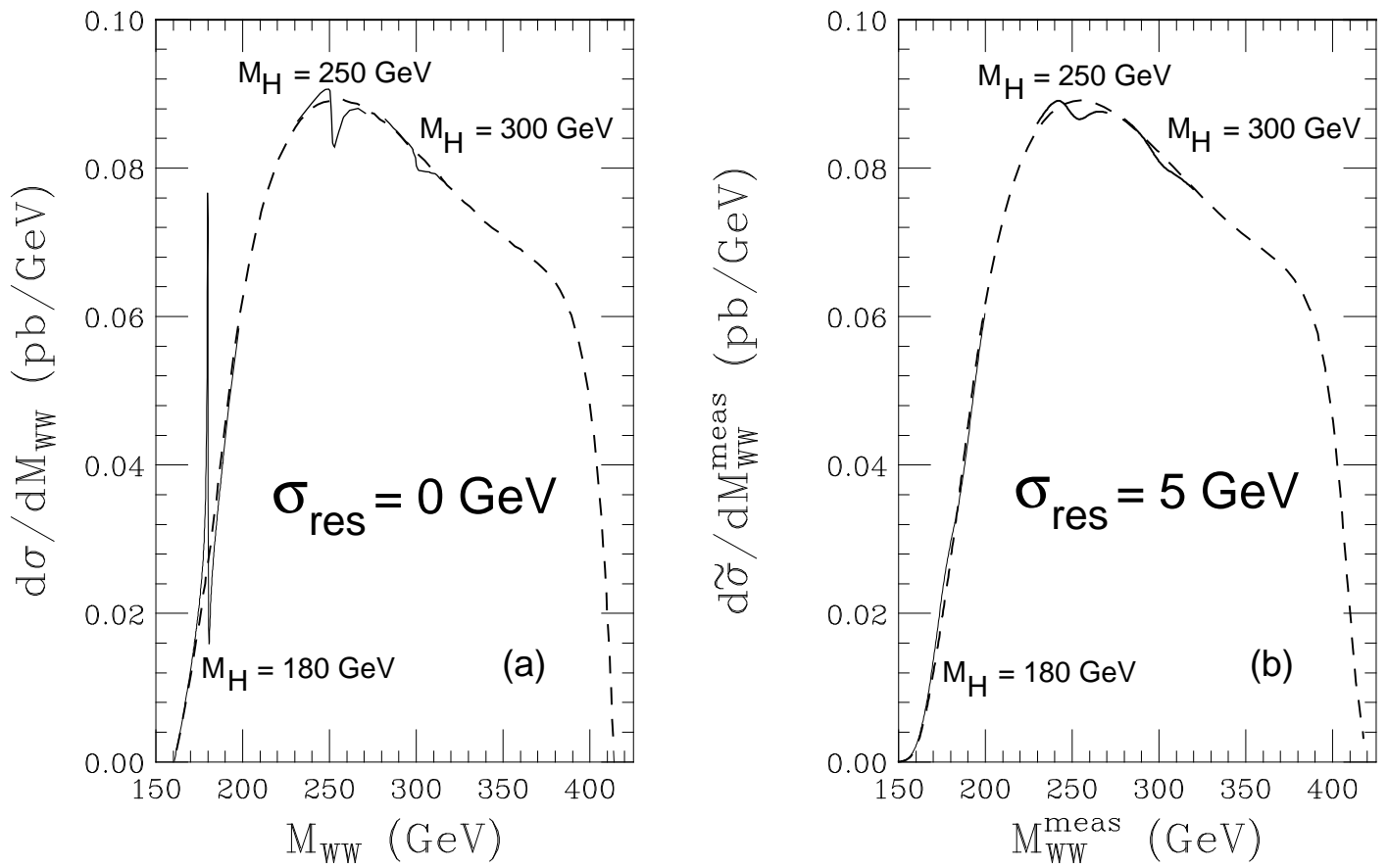


Figure 3

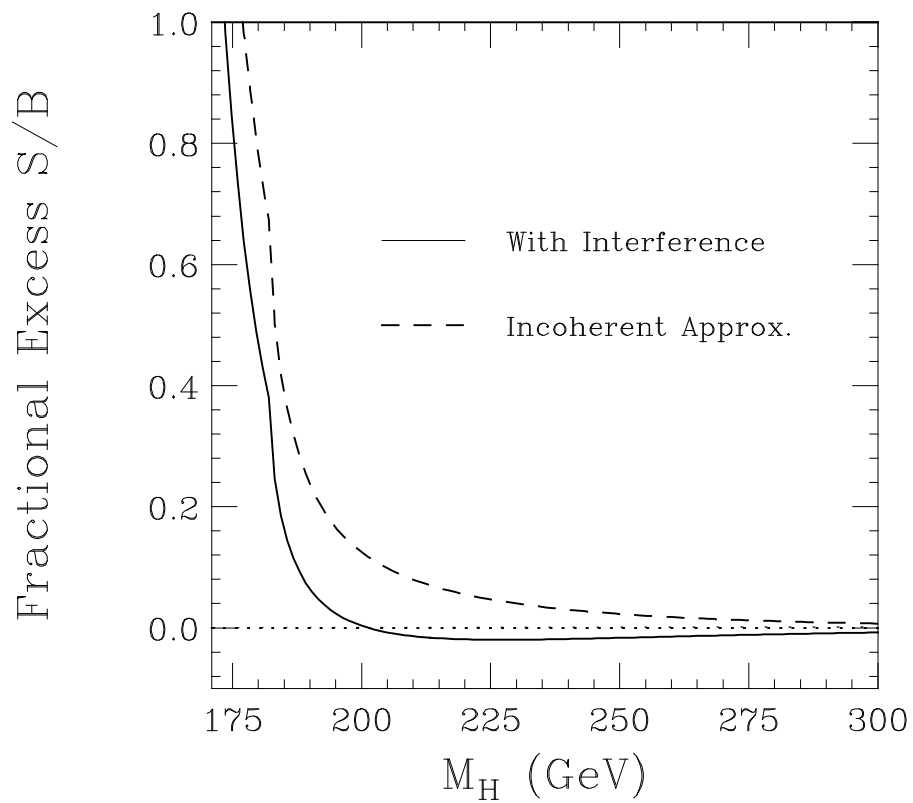


Figure 4